Interpretation of the quasicontinuum band emitted by highly ionized rare-earth elements in the 70—100-Å range

P. Mandelbaum, M. Finkenthal, J. L. Schwob, and M. Klapisch
Racah Institute of Physics, The Hebrew University, 91904 Jerusalem, Israel
(Received 2 September 1986; revised manuscript received 21 January 1987)

Narrow ($\Delta\lambda < 5$ Å), intense quasicontinuum bands, appearing in emission spectra of highly ionized rare-earth elements between 70 and 100 Å, previously observed in tokamaks and laser-produced plasmas, have been obtained from a low-inductance vacuum spark. The bands shift toward shorter wavelengths with increasing atomic number Z. Using the unresolved transition array model, these bands are identified as primarily $4d$-$4f$ transitions in Rh I to Rb I—like ions, although the widths come out too large and the mean wavelengths are much too dependent on ionization stages. Detailed *ab initio* computations show that the interactions between the $4p^6 4d^{N-1} 4f$ and $4p^5 4d^{N+1}$ configurations are responsible for the narrowing and the superposition of the transition arrays for the different ionization stages of a given element, in agreement with experimental data.

I. INTRODUCTION

The spectra emitted in the soft-x-ray range by highly ionized rare-earth elements, obtained from very different sources such as laser-produced plasmas,[1] vacuum sparks (present work), and, recently, tokamak plasmas,[2] show a common feature: a narrow band [less than 5 Å full width at half maximum (FWHM)] is emitted between 70 and 100 Å and its center shifts towards shorter wavelengths as the atomic number Z increases. Since these bands are much brighter than individual lines and still relatively narrow, they could represent excellent soft-x-ray sources for absorption spectroscopy or photolithography. In order to evaluate these potential applications, it is necessary to understand the basic mechanisms underlying the emission, namely, which are the ionization states responsible for the emission, and the transitions involved. O'Sullivan and Carroll[1] have estimated that an ionization stage of about 15 was reached in their laser-produced plasmas. They also have shown[3] that the ground state of the involved ions was $4d^N$. From the scaling of the transition energies with Z and from the ionization states involved, they concluded that $4d$-$4f$ transitions were mainly responsible for these continua.

On the other hand, resolved lines emitted in the same spectral region from rare-earth elements and elements of the fifth row in ionization states neighboring the Pd I sequence, have been extensively studied during recent years. Sugar and Kaufman[4–6] have made a detailed analysis of the Ag I—like (ground state $4d^{10}4f$) and the Pd I—like (ground state $4d^{10}$) transitions in I to Ho spectra. Joshi and van Kleef[7–9] have studied the Rh I—like spectra of the elements of the fifth row, obtained from a vacuum-triggered spark and have analyzed the $4d^9$-$4d^8 5p$ transitions of these ions. Their work was extended by Kaufman, Sugar, and Tech to Xe X, Ba XII, and La XIII.[10–12] However, they did not analyze either the continuum band appearing in these spectra, or the $4d^9$-$4d^8 4f$ transitions in this isoelectronic sequence.

The above-mentioned tokamak spectra obtained under accurately measured electron density and temperature conditions, indicated that even in these hot plasmas, where much higher ionization states were obtained (Zn I— and Cu I—like praseodymium for instance), the continuum bands are still relatively narrow and almost unshifted[2]

This work presents an explanation of the observed emission peaks emitted by these very different sources. It addresses the following questions: Why are the bands still narrow, even when as many as ten different ionization states are involved, as in the case of tokamak spectra? Also, which are the transitions responsible for the large number of unresolved intense lines which might produce these continuum features regardless of the spectrometer resolution? Although, in the present work, vacuum spark spectra of several rare-earth elements have been recorded in the range considered, the emphasis is on a general explanation of the vacuum spark spectra as well as spectra obtained from higher-temperature sources such as tokamaks and high-power laser-produced plasmas.

The structure of the paper is as follows. Section II describes the experimental data obtained in the present work. Section III presents the theoretical interpretation of the spectra: a first part briefly describes the results of two theoretical approaches—the configuration average model and the unresolved transition array (UTA) method[13–16]—considered first by the authors. Since neither led to results in good agreement with the experiment, detailed level computations including configuration interactions have been performed. The second part of this section presents computations for five ionization states of praseodymium. It is shown that these interactions are strong enough to cause a profound alteration of the line distribution inside the bands. As a result, it is shown in the third paragraph of this section, that significant shift and narrowing of the bands are predicted. Section IV discusses the comparison of the theoretical results with experiment for La to Nd.

II. EXPERIMENTAL DATA

Spectra of La, Ce, Pr, and Nd have been obtained from a low-inductance vacuum-spark source.[17] Anodes of pure

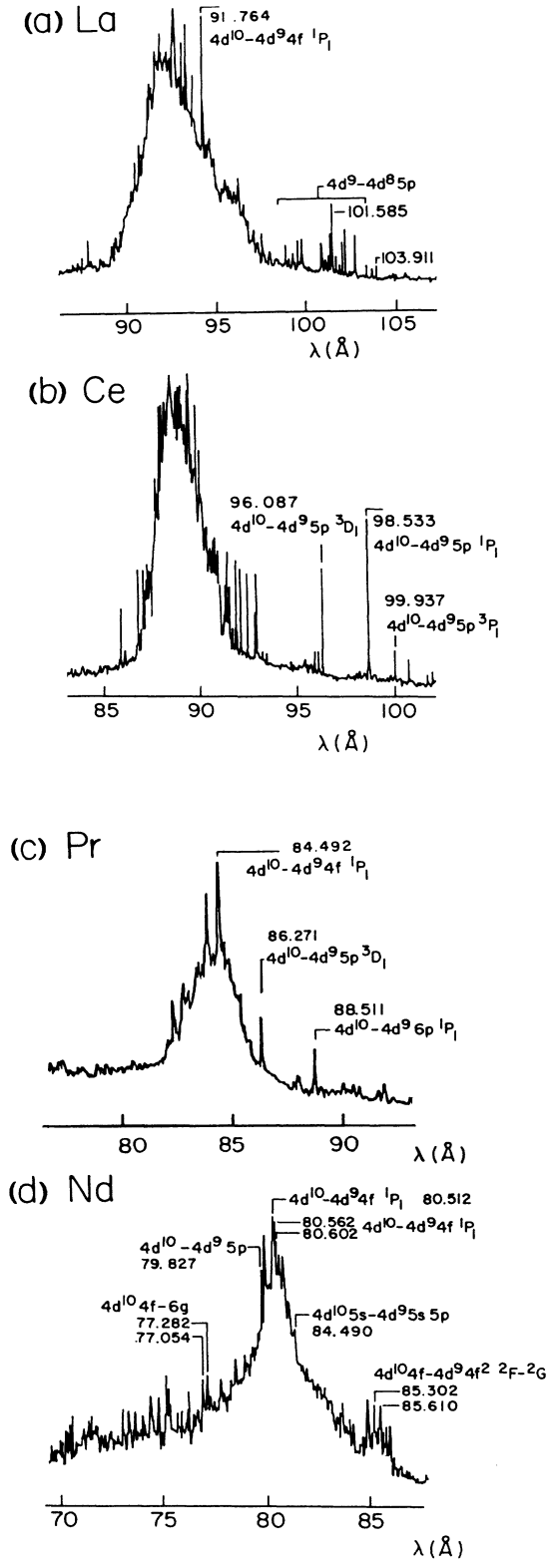

FIG. 1. Microphotometer tracing of the observed La, Ce, Pr, and Nd spectra emitted from a vacuum spark in the 70—100-Å region. Indicated lines were identified in Refs. 4—6.

rare-earth elements have been used. The spectra were recorded on Kodak SC5 or Ilford Q2 plates by means of a 2-m grazing-incidence Schwob-Fraenkel spectrograph.[18] Bausch & Lomb ruled gratings with 600 and 1200 lines per mm, interferometrically adjusted on the Rowland circle, have been used to cover the spectral range of interest. Some of the previously identified rare-earth lines,[4–6] together with superimposed Al lines, have been used as standards and led to a wavelength accuracy better than 0.005 Å. (Lines emitted by ions having simple ground configurations have been measured to compare our results with those obtained in previous experiments.) In general, the spectra are similar to those obtained with a very high resolution by Sugar and Kaufman.[4–6] These spark spectra are also quite comparable to those obtained by O'Sullivan and Caroll from laser-produced plasmas using compounds of the rare-earth elements, as far as the center and the width of the continua are concerned. Figure 1 presents the spectra of La to Nd spectra obtained in the present work in the 70—100-Å region. Previously identified lines of the Rh I, Pd I, and Ag I isoelectronic sequences[4–6,12] have been indicated. Two features are obvious: The center of the bands shifts towards shorter wavelengths (as observed by O'Sullivan and Caroll) and the bands become narrower, as Z increases.

III. THEORETICAL INTERPRETATION OF THE SPECTRA

In all the theoretical models considered here, level energies and line strengths are calculated *ab initio* using the relativistic RELAC code.[19]

A. The configuration average and UTA models

The simplest way to predict the position of an array of spectral lines obtained from transitions between two configurations having a large number of levels is to calculate the mean transition energy, i.e., the difference of the average energies of the two configurations involved. In this method no attention is paid to the spread of the transition array. The mean wavelength of the $4d^9$-$4d^8 4f$ transition is predicted by this kind of calculation at 102.6 Å for Pr XV, about 18 Å off from the center of the observed narrow band at 84 Å. This discrepancy comes from the fact that configuration average energies ignore transition selection rules.[20,21] The selection rules are bound to cause a shift between observed and configuration-average computed transition energies.

An analytical expression for this shift has been given in the framework of the UTA (unresolved transition array) model developed by Bauche-Arnoult, Bauche, and Klapisch.[13–16] In this model, which takes into account the line strength of the transitions, simple analytical expressions are obtained for the mean value $\overline{E}$ and for the variance σ^2 (and in some special cases for the asymmetry) of the weighted distribution of the individual transition energies E_{ij} (the weight of each transition being the electric dipole line strength S_{ij}). From these quantities, $\overline{E}$ and σ^2, one can define the mean wavelength $\overline{\lambda}$ and the spectral width $\Delta\lambda$ of the transition array (which would correspond to the FWHM for a Gaussian profile) as follows:

$$\bar{\lambda} = 10^8/\bar{E}\ , \tag{1}$$

$$\Delta\lambda = 2.355\times 10^8\sigma/\bar{E}^{\,2}\ , \tag{2}$$

where $\bar{E}$ and σ are expressed in cm^{-1} and $\bar{\lambda}$ and $\Delta\lambda$ in Å.

Figure 2 illustrates the results obtained by the two models for the $4d^N$-$4d^{N-1}4f$ arrays of praseodymium (curve 1: average configuration model; curve 2: UTA model). Clearly, the two results are very different: The first approach predicts a nearly constant wavelength with increasing ionization state, whereas the second one gives an increasing mean wavelength. The UTA model seems to better describe the experiment for the lower ionization states: In the case of the Pr XV $4d^9$-$4d^8 4f$ transition, for instance, the first model gives a mean wavelength of 102.6 Å, and the second one predicts it at 81.8 Å, close to the experimental band observed at 84 Å. The remaining difference of 2 Å may be attributed to the overestimation

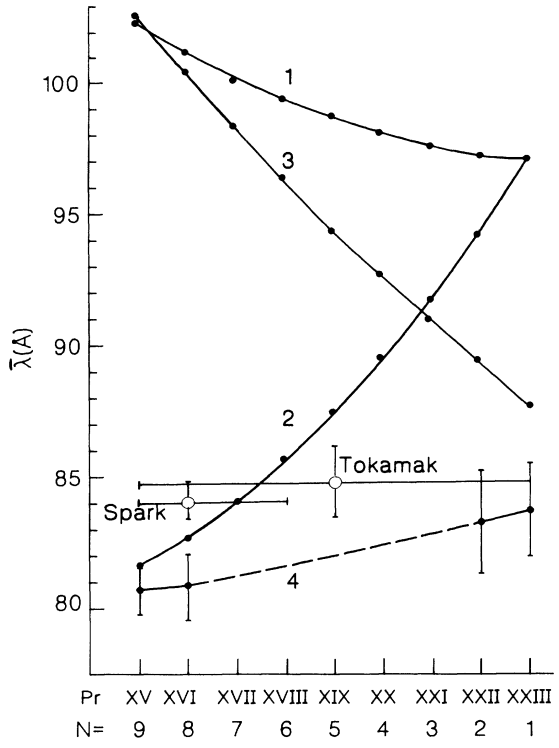

FIG. 2. Mean wavelength of Pr transition arrays as a function of the ionization state or the number N of $4d$ electrons in the ground state. Curve 1: for $4d^N$-$4d^{N-1}4f$, calculated from the difference of the average configuration energies. Curve 2: for $4d^N$-$4d^{N-1}4f$, obtained from line-strength weighted average calculations (UTA model). Curve 3: for $4p^6 4d^N$-$4p^5 4d^{N+1}$, obtained from line-strength weighted average calculations (UTA model). Curve 4: from *ab initio* full calculations, for four ionization states, introducing configurations mixing between the two types of transitions. Vertical bars indicate the apparent spectral width (for $w = a$). ⊣◇⊢: experimental data from vacuum-spark and tokamak spectra. Vertical bars indicate the width (FWHM) of the emission bands, and horizontal bars represent the ionization states present in the plasma.

of the exchange integrals. However, the UTA model fails in some important aspects: first, it yields for the calculated width of the $4d^9$-$4d^8 4f$ array in Pr XV a value of about 5 Å. This is about twice the width of the band in our experimental vacuum-spark spectra. Second, this model predicts a quite steep increase in the mean wavelength of the $4d^N$-$4d^{N-1}4f$ transitions when the ionization state increases, as shown by curve 2 in Fig. 2. This would imply an even wider array in our spectra, since several ionization states are expected to be present, and a displaced band for more highly ionized plasmas. However, this has not been observed in tokamak plasmas where ionization states as high as Cu I— and Zn I—like ones have been identified.

In order to try to interpret the experimental results, UTA model computations have been performed also for transitions involving other upper configurations, especially for the $4p^6 4d^N$-$4p^5 4d^{N+1}$ transition array. Curve 3 in Fig. 2 represents the results for Pr. This shows, in contrast to curve 2, a decrease of the mean wavelength as a function of the ionization state. These results also cannot explain the experimental data.

B. Individual line computations including configuration interactions

The above discrepancies can be explained by strong configuration-interaction effects which cannot be yet included in the UTA model. Therefore, in order to take into account these effects, individual line calculations of the entire arrays had to be performed, much like the classical works of Cowan and co-workers.[22,23] This was done by using the RELAC code to compute the radial integrals, and a modified version[24] of the MCP code[25] for the angular coefficients. Using this method, *ab initio* calculations including configuration interaction were performed for all the elements from La to Eu. In the following, only the results for the case of Pr are discussed in detail.

In order to evaluate the accuracy of the computation method, theoretical predictions and experimental results were compared within the simple Pd I isoelectronic sequence (ground state $4d^{10}$) for elements from I to Nd. The conclusion of this comparison, illustrated in Table I for the Pr XIV case, is that the computed energy levels belonging to the excited configuration $4d^9 5p$ are accurate within 1%, whereas the energy of the ^1P level of the configuration $4d^9 4f$ is overestimated by up to 4%. This gives an indication of the absolute accuracy which can be expected. These results are similar to those of Sugar and

TABLE I. The Pd I—like transitions in Pr XIV. Comparison is made between experiment (Ref. 6) and calculations (present work).

Transition	Level	λ_{expt} (Å)	λ_{theor} (Å)
$4d^{10}$-$4d^9 5p$	$^1P_1$	88.511	87.806
	$^3P_1$	89.771	89.115
	$^3D_1$	86.271	85.627
$4d^{10}$-$4d^9 4f$	$^1P_1$	84.492	81.336
	$^3D_1$	104.225	104.300

Kaufman[6] who used an effective G^1 integral 0.75 times the Hartree-Fock value.

It should be pointed out that in the Pd I isoelectronic sequence, configuration interaction involving $4d^9 4f$ is expected mainly with $4d^9 5p$. For this sequence there is no possible interaction with configurations of the type $4p^5 4d^{N+1}$ (since the $4d^{10}$ subshell is full in the ground state). Also, there are only three transitions form $4d^9 4f$ to the ground and it is therefore possible to analyze in detail the evolution of the level mixing along the sequence, as done by Sugar and Kaufman. These authors have described,[6] for instance, the effect of the configuration interaction on the $4d^9 5p$ and $4d^9 4f\ ^1P_1$ levels. They found a mixture of 4.5% in Pr XIV, whereas for the neighboring Nd XV it reaches 20%. This fact is well reproduced by the present *ab initio* calculations.

In the other sequences having an open $4d^N$ subshell in the ground state, mixing between $4p^6 4d^{N-1} 4f$ and $4p^5 4d^{N+1}$ has to be considered. But, as the $4d^N$ subshell opens, the configuration involved becomes more and more complex; for this reason, only the simpler ionic species isoelectronic to Rh I (ground $4d^9$) and Ru I (ground $4d^8$) for the lower ionization states, and to Sr I (ground $4d^2$) and Rb I (ground $4d$) for the higher ionization states, have been studied here. The results should, however, allow us to predict the general trends of the spectra for all the isoelectronic sequences.

First, the calculations for the Rh I–like Pr XV ion are presented. Results for the most intense lines of the $4p^6 4d^9$-$4p^6 4d^8 4f$ transition array are given in Table II. In this table, the upper level is given a shortened jj notation: j_1 and j_2 are the j quantum numbers of the two $4d$ holes and J_{4f} is the j value of the $4f$ outer electron. The two quantum numbers j_1 and j_2 couple to J_{4d} which in turn couples with J_{4f} to give the total quantum number J of the upper level. The quantum number J_G of the ground configuration is given in the next column. Computed wavelengths (in Å) and oscillator strengths are given in the two next columns. The coefficient in front of the upper level designation is the square of the eigenvector amplitude, the sign being determined by the following phase convention: The maximum amplitude of the large component of the Dirac one-electron wave functions has to be positive. Only the dominant component is shown for $4d^8 4f$. The coupling is far from any simple pure scheme.

Part (a) of Table II gives those lines which arise from $4p^6 4d^8 4f$ levels with $J = \frac{5}{2}, \frac{7}{2}$. These transitions are not affected by the introduction of the $4p^5 4d^{10}$ configuration ($J = \frac{1}{2}, \frac{3}{2}$) in the computation, and since these transitions are the strongest (notice the very large gf's), the main part of the array is not changed. This explains why the mean wavelength calculated with the UTA model gave acceptable results for this sequence.

TABLE II. Results of calculations for the most intense lines of the Pr XV $4p^6 4d^9$-$4p^6 4d^8 4f$ transitions: (a) Transitions arising from $J = \frac{5}{2}, \frac{7}{2}$ levels which are not changed by the introduction of $4p^5 4d^{10}$ in the calculations. (b) Transitions arising from $J = \frac{1}{2}, \frac{3}{2}$ without $4p^5 4d^{10}$ mixing. (c) As part (b) but with $4p^5 4d^{10}$ mixing.

(a)

Upper level $x[(j_1,i_2)J_{4d},J_{4f}]$	J	J_G	λ (Å)	gf
$0.31[(\frac{3}{2},\frac{3}{2})2,\frac{5}{2}]$	$\frac{5}{2}$	$\frac{3}{2}$	80.545	20.0
$0.38[(\frac{5}{2},\frac{5}{2})4,\frac{7}{2}]$	$\frac{5}{2}$	$\frac{5}{2}$	81.373	18.2
$0.25[(\frac{5}{2},\frac{5}{2})2,\frac{7}{2}]$	$\frac{7}{2}$	$\frac{5}{2}$	80.473	27.0

(b)

Upper level $x[(j_1,j_2)J_{4d},J_{4f}]$	J	J_G	λ (Å)	gf
$0.62[(\frac{3}{2},\frac{5}{2})4,\frac{7}{2}]$	$\frac{1}{2}$	$\frac{3}{2}$	87.173	4.4
$0.35[(\frac{3}{2},\frac{3}{2})2,\frac{5}{2}]$	$\frac{3}{2}$	$\frac{3}{2}$	81.788	11.4
$0.38[(\frac{3}{2},\frac{5}{2})4,\frac{5}{2}]$	$\frac{3}{2}$	$\frac{5}{2}$	86.040	8.4

(c)

Upper level $x[(j_1,j_2)J_{4d},J_{4f}]+y(4p_j^5 4d^{10})$	J	J_G	λ (Å)	gf
$0.41[(\frac{3}{2},\frac{5}{2})4,\frac{7}{2}]-0.39(4p_{1/2}^5 4d^{10})$	$\frac{1}{2}$	$\frac{3}{2}$	78.677	6.9
$0.36[(\frac{3}{2},\frac{3}{2})2,\frac{5}{2}]+0.02(4p_{3/2}^5 4d^{10})$	$\frac{3}{2}$	$\frac{3}{2}$	81.652	12.3
$-0.37[(\frac{3}{2},\frac{5}{2})4,\frac{5}{2}]-0.18(4p_{3/2}^5 4d^{10})$	$\frac{3}{2}$	$\frac{5}{2}$	80.880	13.4

The $J=\frac{1}{2},\frac{3}{2}$ levels of $4p^6 4d^8 4f$, however, mix strongly with $4p^5 4d^{10}$. This is the case for two of the three more intense transitions with $J=\frac{1}{2}$ and $\frac{3}{2}$ considered in parts (b) and (c) of Table II; part (b) presents the results without taking into account the $4p^5 4d^{10}$ levels and part (c) when the mixing due to these levels is introduced in the computations. A consequence of this mixing is a redistribution of the wavelengths and intensities of the weaker lines. These results are shown in Fig. 3, where results of full *ab initio* computations for Pr XV are presented, by means of synthetic plots. In these plots, the height of each spectral line is proportional to the line strength. Since there are hundreds of lines, a Gaussian profile with an arbitrary width (FWHM) of 0.2 Å has been introduced for each line, in order to visualize the resulting intensity distribution within the emitting features. The synthetic spectrum (a) in Fig. 3 is obtained when the pure $4p^6 4d^N$-$4p^6 4d^{N-1} 4f$ array is considered. Spectrum (b) corresponds to the pure $4p^6 4d^N$-$4p^5 4d^{N+1}$ array normalized to the same height. (c) is the superposition of these two spectra with proper relative strengths, and (d) is obtained from complete configuration interaction computations by diagonalization of the energy matrices. Figures 4,5, and 6 present the same type of computed spectra for Ru I—, Sr I—, and Rb I—like praseodymium. In each case an important narrowing of the emitting feature is observed

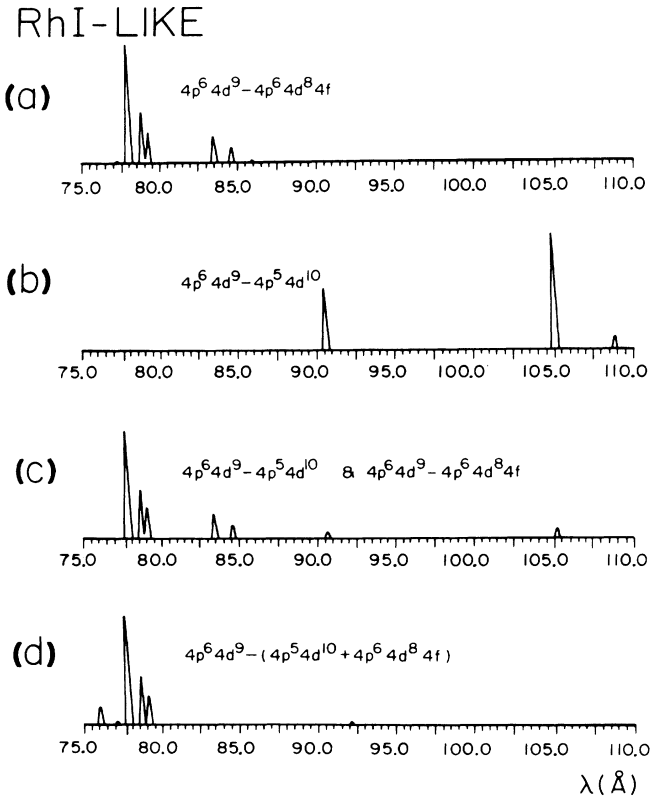

FIG. 3. Synthetic plots of the different computed arrays for Pr XV (Rh I—like, $N=9$). (a) Pure $4p^6 4d^N$-$4p^6 4d^{N-1} 4f$ transitions. (b) Pure $4p^6 4d^N$-$4p^5 4d^{N+1}$ transitions. (c) Superposition of (a) and (b). (d) Mixed $4p^6 4d^N - (4p^6 4d^{N-1} 4f + 4p^5 4d^{N+1})$ transitions.

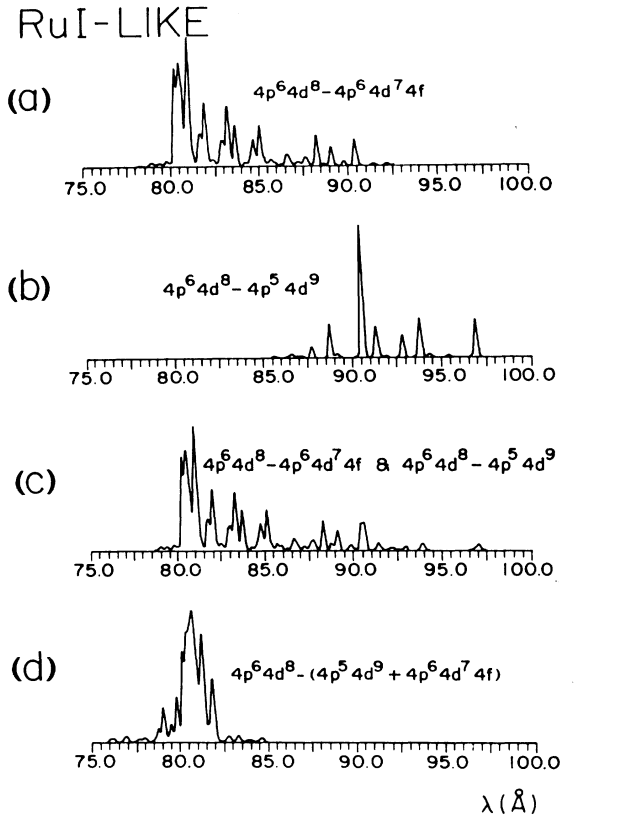

FIG. 4. Synthetic plots of the different computed arrays for Pr XVI (Ru I—like, $N=8$).

when mixing is included, with the long wavelength part nearly disappearing. It can be noticed that for the higher ionization states the entire resulting array is shifted towards shorter wavelengths, compared to pure $4d^N$-$4d^{N-1} 4f$ transition array.

As a byproduct of the calculations in the Rh I sequence a remark has to be made: Because of the strong mixing, there is a noticeable decrease of intensity of the $4p^6 4d^9$-$4p^5 4d^{10}$ lines. This can explain the difficulties encountered in the classification of these lines in this isoelectronic sequence. Also, it has to be noted that when introducing the mixing with the $4p^6 4d^8 5p$ configuration, which is close to $4p^6 4d^8 4f$ precisely for Pr, no appreciable change was observed in the general structure of the synthetic transition array. This is due to the fact that the mixing coefficients for these two configurations are relatively small.

C. Shift and narrowing of the transition arrays

The general trend observed in the praseodymium synthetic spectra discussed above—i.e., the wavelength shift of the emitting feature with respect to the pure $4d^N$-$4d^{N-1} 4f$ spectrum and the narrowing of the transition arrays when configuration mixing was included in the calculations—has been systematically studied along the isoelectronic sequences from La to Eu. In order to com-

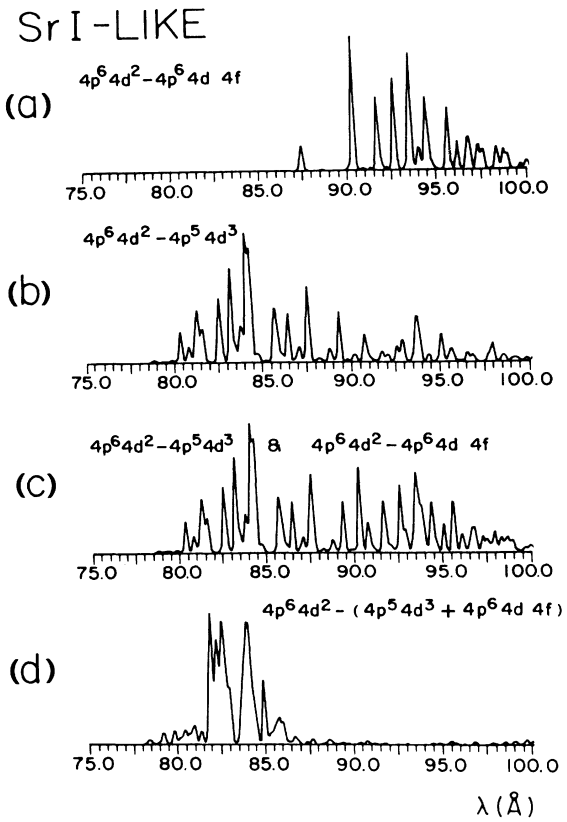

FIG. 5. Synthetic plots of the different computed arrays for Pr XXII (Sr I—like, $N=2$).

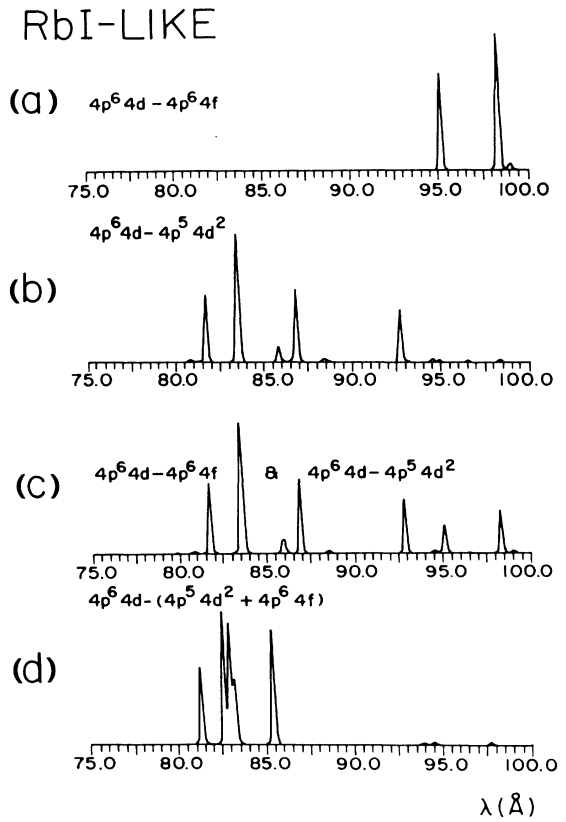

FIG. 6. Synthetic plots of the different computed arrays for Pr XXIII (Rb I—like, $N=1$).

pare these theoretical results with experimental spectra, line-strength-weighted mean wavelengths and apparent spectral widths of the arrays were calculated using the computed data for individual lines (unlike the UTA model).

The weighted mean wavelengths obtained are given in Table III for the four isoelectronic sequences considered. The results for praseodymium are represented by curve 4 in Fig. 2. This shows, in particular, that configuration-mixing computations predict a very small variation of $\bar{\lambda}$ as a function of the ionization state (from Rh I to Rb I sequence), in contrast to previous results considering one type of transition only. For instance, for Pr XV to Pr XXIII, $\bar{\lambda}$ varies only from 80.7 to 83.8 Å, instead of from 81.8 to 97.1 Å assuming $4d^N$-$4d^{N-1}4f$ transitions only, and from 103.2 to 85.5 Å for pure $4p^6 4d^N$-$4p^5 4d^{N+1}$.

The synthetic spectra [Figs. 3(d)—6(d)] which show a bunching together of the intense lines around $\bar{\lambda}$, include, however, a great number of weak lines (not visible in the plots) spread quite far away. Therefore the spectral variance is not adequate to describe here the apparent width of the main emitting feature, since the contribution of the weak lines is overestimated due to the fact that the wavelength differences are squared in the variance calculation. Consequently, the following procedure has been made in order to estimate the apparent width of the array: The spectral width $\Delta\lambda$ has been calculated from expression (2) but considering only the lines inside a limited spectral range $\bar{\lambda} \pm w$, where w is a variable parameter. Figures 7 (a)—(c) present the plots of $\Delta\lambda$ as a function of w for Pr ions. Curves 1 represent the results for the dominant unmixed transition ($4d^N$-$4d^{N-1}4f$ for Pr XV and Pr XVI, and $4p^6 4d^N$-$4p^5 4d^{N+1}$ for Pr XXII), while curves 2 are for the mixed arrays. One notices a quasiplateau in curves 2 for $w=a$ at about 10 Å; this corresponds thus to the apparent spectral width ($\Delta\lambda_a$) of the array. This apparent width is much smaller than the computed total width, which would be meaningful for a line array distribution without configuration interaction. This effect is indeed not observed in curves 1. The same apparent narrowing of the array width due to configuration interaction, has been predicted for the other rare-earth elements; the results are illustrated in Figs. 7(d)—7(f) and reported in Table III. In the case of Pr, for instance, one predicts that $\Delta\lambda_a$ varies from about 2 to 4 Å for the four ionization states considered, whereas computations for pure $4d$-$4f$ and $4p$-$4d$ transitions give a width between 4 and 8 Å and between 9 and 16 Å, respectively. The apparent spectral widths obtained from the configuration-mixing calculations are represented by the vertical bars on curve 4 in Fig. 2.

TABLE III. Theory: Calculated line-strength weighted mean wavelength and apparent spectral width for pure $4d^N$-$4d^{N-1}4f$ and $4p^64d^N$-$4p^54d^{N+1}$ transitions, and for configuration mixing. Experiment: Observed peak wavelength and width (FWHM) of the bands.

	La		Ce		Pr		Nd		Pm		Sm		Eu	
	$\bar{\lambda}$ [a]	$\Delta\lambda_a$ [b]	$\bar{\lambda}$	$\Delta\lambda_a$	$\bar{\lambda}$	$\Delta\lambda_a$	$\bar{\lambda}$	$\Delta\lambda_a$	$\bar{\lambda}$	$\Delta\lambda_a$	$\bar{\lambda}$	$\Delta\lambda_a$	$\bar{\lambda}$	$\Delta\lambda_a$
						Theory								
$4d$-$4f$														
Rh I	90.57	5.56	85.89	5.24	81.76	4.95	78.12	4.69	74.85	4.45	71.86	4.23	69.13	4.03
Ru I	91.29	7.57	86.83	7.15	82.85	6.79	79.29	6.44	76.07	6.14	73.14	5.88	70.15	5.63
Sr I	102.25	8.40	98.10	8.10	94.28	7.82	90.79	7.59	87.51	7.46	84.49	7.29	81.64	7.12
Rb I	105.23	3.58	100.99	3.66	97.09	3.73	93.48	3.81	90.16	3.90	87.03	3.98	84.17	4.07
$4p$-$4d$														
Rh I	113.24	16.27	109.02	16.38	103.22	16.49	98.77	16.62	94.63	16.76	90.78	16.90	87.18	17.03
Ru I	112.05	12.98	106.98	13.03	102.14	13.28	97.96	13.32	94.64	12.17	91.66	12.98	88.15	13.06
Sr I	94.97	11.81	90.74	11.63	86.82	11.10	83.13	10.65	79.87	10.58	76.59	10.46	73.41	9.97
Rb I	93.30	9.48	89.26	9.00	85.52	8.78	81.93	8.32	78.53	7.89	75.38	7.92	73.34	7.57
Mixing														
Rh I	89.37	1.99	84.79	1.82	80.74	1.70	77.16	1.64	73.94	1.60	70.99	1.58	68.30	1.57
Ru I	88.92	2.59	84.27	2.44	80.79	2.33	77.34	2.27	74.21	2.26	71.35	2.26	68.69	2.25
Sr I	90.62	3.84	86.85	3.90	83.35	4.11	80.09	4.47	77.00	4.78	74.12	5.13	71.36	5.39
Rb I	91.13	3.01	87.32	3.32	83.79	3.77	80.40	3.74	77.28	4.31	74.24	4.27	71.42	4.66
	λ Peak	$\Delta\lambda$ FWHM	λ Peak	$\Delta\lambda$ FWHM	λ Peak	$\Delta\lambda$ FWHM	λ Peak	$\Delta\lambda$ FWHM						
						Experiment								
Spark[c]	92.9	4.3	89.0	2.9	84.2	2.6	80.2	3.0						
Tokamak[d]					84.8	3.4								

[a]Wavelengths and spectral widths in Å.
[b]Summation range $\bar{\lambda}\pm10$ Å.
[c]Present work.
[d]Finkenthal *et al.*, Ref. 2.

IV. COMPARISON WITH EXPERIMENT

The combined effect of these two new theoretical results—the narrowing of the transition arrays, together with the almost constant mean wavelength $\bar{\lambda}$ as a function of the ionization state—enables us to interpret very well the strikingly narrow continuum bands observed in the experimental spectra [Figs. 1(a)—1(d)], in spite of the superposition of emissions from several ionization states for each element. The measured peak wavelengths of the La to Nd bands emitted from the vacuum-spark and of Pr observed in tokamak plasma[2] are given in Table III. The experimental width (FWHM) for each emission band is also reported in this table; it should be noted that these values are not very accurate because of the non-Gaussian and somewhat irregular shape of the spectral profile. One notices in Table III that the theoretical values obtained from configuration-mixing computations compare quite well with the experimental data, even though in the present model the line strength is introduced for each transition within the array, instead of the line intensity.

The experimental results for praseodymium are reported in Fig. 2, where the two experimental points correspond to the peak wavelength of the bands observed in the vacuum spark and the tokamak plasma, respectively. Vertical bars indicate the experimental width (FWHM) of the band and horizontal bars represent the ionization states which are present inside the plasma. In the vacuum spark, only the lower ionization states of the $4d^N$ configurations are produced, whereas the conditions prevailing in the tokamak plasma enable all the ionization states ($N=9$ to 1) (see Ref. 2) to be reached. Thus, the observed bands in this plasma actually represent the superposition of the peaks emitted from the successive ions. This can explain the slightly wider Pr band in the tokamak spectrum ($\Delta\lambda\approx3.4$ Å), compared to that obtained from the spark (2.6 Å). The relatively wider band observed in the spark spectra for lanthanum compared with neodymium (see Fig. 1) can also be attributed to the presence of higher ionization states in the spark plasma in the case of lower Z elements.

The fact that the experimental bands are relatively narrow, and moreover, that there is only a very small wavelength shift of the peak from the spark spectrum to that of the tokamak, where a quite different ionization state distribution exists, is in good agreement with the present

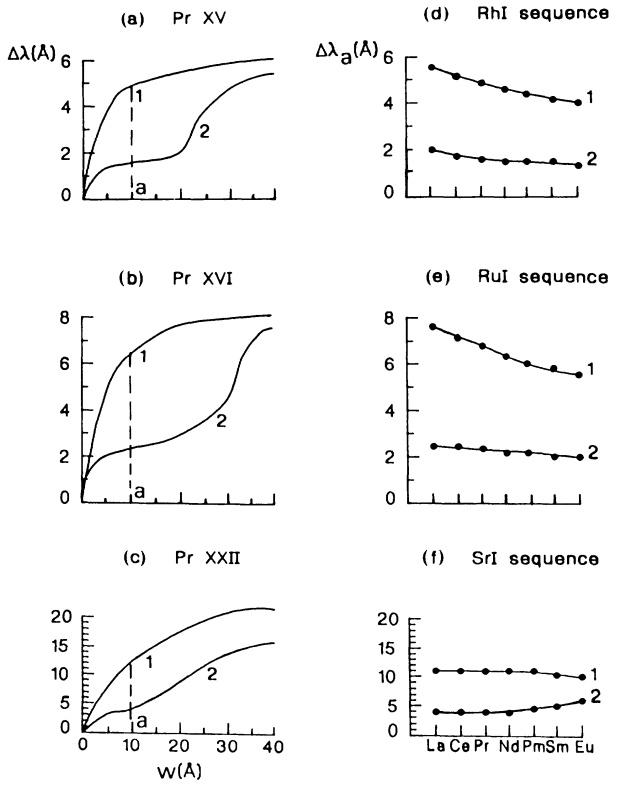

FIG. 7. (a)—(c) Spectral width of the transition arrays for Pr, calculated in the range $\bar{\lambda} \pm w$ as a function of w, where $\bar{\lambda}$ is the line-strength weighted mean wavelength. Curve 1: Only the dominant transition is considered: $4d^N$-$4d^{N-1}4f$ for the cases (a) and (b), and $4p^6 4d^N$-$4p^5 4d^{N+1}$ for (c). Curve 2: Configuration mixing of $4d^N$-$4d^{N-1}4f$ and $4p^6 4d^N$-$4p^5 4d^{N+1}$ is introduced. (a) $N=9$ (Rh I—like ion). (b) $N=8$ (Ru I—like ion). (c) $N=2$ (Sr I—like ion). (d)—(f) Apparent spectral width of the transition arrays showing the narrowing due to configuration mixing (curves 2) along the Rh I, Ru I, and Sr I isoelectronic sequences [curves 1 have the same meaning as in (a), (b), and (c)].

computations, regarding both the trend shown by curve 4 and the indicated spectral widths. The discrepancy remaining between the absolute values of $\bar{\lambda}$ is probably due to the *ab initio* calculation method, as discussed above in the test case of the well-separated Pd I—like lines

V. CONCLUSION

The present work explains the nature, the position, and the spectral width of the quasicontinuum bands observed in the soft-x-ray spectra of the rare-earth elements. It has been shown, by performing *ab initio* level structure computations, that the effect of configuration interaction between the excited $4p^5 4d^{N+1}$ and $4p^6 4d^{N-1}4f$ states in various ionization states leads to a strong narrowing of the emission array originating from transitions between these levels and the ground $4p^6 4d^N$. As a result, the above-mentioned quasicontinuum, produced by a very large number of lines (thousands for each ion for $N=3$ to 7), emitted within a spectral interval of 2—4 Å, is created. Moreover, for a given element, with the changing of the ionization state, the band is only slightly shifted. Thus, even if as many as ten ions are emitting lines belonging to these transitions, the entire emission remains centered in a narrow band around a fixed spectral position. These results, predicted theoretically by the present work, have been well confirmed by previously recorded laser and tokamak spectra, and by the vacuum-spark spectra obtained in the present work.

The observation of these narrow intense emission bands can lead to interesting applications in photoexcitation experiments, such as optical pumping for soft-x-ray and extreme-uv (XUV) lasers.[26] As the Z of the elements involved increases, the entire band shifts towards shorter wavelengths. Besides, the bands of adjacent elements appear to be juxtaposed, covering continuously an extended spectral range, thus giving rise to a bright tunable XUV source. The paper presents the experimental observation of four peaks covering the range from 78—96 Å, but using other (especially higher-Z) elements, it should be possible to cover the 50—100-Å domain.

ACKNOWLEDGMENTS

The authors wish to thank P. K. Caroll and co-workers at the University College of Dublin, who first brought to their attention this challenging problem of the rare-earth quasicontinua. Enlightening discussions on the subject with G. O'Sullivan, J. Sugar, V. Kaufman, C. Bauche-Arnoult, and J. Bauche are acknowledged. One of the authors (M.F.) acknowledges the Revson foundation for support in this research.

[1]G. O'Sullivan and P. K. Caroll, J. Opt. Soc. Am. **71**, 227 (1981).
[2]M. Finkenthal, S. Lippman, L. K. Huang, T. L. Yu, B. C. Stratton, H. W. Moos, M. Klapisch, P. Mandelbaum, and A. Bar-Shalom, J. Appl. Phys. **59**, 3644 (1986).
[3]P. K. Caroll and G. O'Sullivan, Phys. Rev. A **25**, 508 (1982).
[4]J. Sugar and V. Kaufman, Phys. Scr. **24**, 742 (1981).
[5]V. Kaufman and J. Sugar, J. Opt. Soc. Am. B **1**, 38 (1984).
[6]J. Sugar and V. Kaufman, Phys. Scr. **26**, 419 (1982).
[7]Th. A. M. van Kleef and Y. N. Joshi, J. Opt. Soc. Am. **69**, 132 (1979).
[8]Y. N. Joshi and Th. A. M. van Kleef, J. Opt. Soc. Am. **70**, 1344 (1980).
[9]Th. A. M. van Kleef and Y. N. Joshi, J. Opt. Soc. Am. **71**, 55 (1981).
[10]V. Kaufman, J. Sugar, and J. L. Tech, J. Opt. Soc. Am. **73**, 691 (1983).
[11]J. Sugar, J. L. Tech, and V. Kaufman, J. Opt. Soc. Am. **73**,

1077 (1983).
[12]J. L. Tech, V. Kaufman, and J. Sugar, J. Opt. Soc. Am. B **1**, 41 (1984).
[13]C. Bauche-Arnoult, J. Bauche, and M. Klapisch, Phys. Rev. A **20**, 2424 (1979).
[14]C. Bauche-Arnoult, J. Bauche, and M. Klapisch, Phys. Rev. A **25**, 2641 (1982).
[15]J. Bauche, C. Bauche-Arnoult, E. Luc-Koenig, J. F. Wyart, and M. Klapisch, Phys. Rev. A **28**, 829 (1983).
[16]C. Bauche-Arnoult, J. Bauche, and M. Klapisch, Phys. Rev. A **31**, 2248 (1985).
[17]J. L. Schwob and B. S. Fraenkel, Phys. Lett. **40A**, 81 (1972).
[18]A. Filler, J. L. Schwob, and B. S. Fraenkel, in *Proceedings of the Fifth International Conference on the Vacuum Ultraviolet Radiation Physics,* edited by M. C. Castex, M. Pouey, and N. Pouey (Centre National de la Recherche Scientifique, Paris, 1977), Vol. III, p. 86.
[19]M. Klapisch, J. L. Schwob, B. S. Fraenkel, and J. Oreg, J. Opt. Soc. Am. **67**, 148 (1977).
[20]M. Klapisch, in *Proceedings of the Vth General Conference of EPS, Istanbul, 1981,* edited by I. A. Dorobantu (The Central Institute of Physics, Bucharest, 1982), p. 384.
[21]M. Klapisch, J. Bauche, and C. Bauche-Arnoult, in The Spectroscopy of Unresolved Transition Arrays in Highly Ionized Atoms [Phys. Scr. T **3**, 224 (1983).
[22]R. D. Cowan, *The Theory of Atomic Structure and Spectra* (University of California, Berkeley, 1981).
[23]R. C. Isler, R. V. Neidigh, and R. D. Cowan, Phys. Lett. **63A**, 295 (1977).
[24]A. Bar-Shalom and M. Klapisch, Comput. Phys. Commun. (to be published).
[25]I. P. Grant, B. J. McKenzie, P. H. Norrington, D. F. Mayers, and N. C. Pypers, Comput. Phys. Commun. **21**, 207 (1980).
[26]M. Finkenthal, J. L. Schwob, and P. Mandelbaum, in Proceedings of the International Colloquium on XUV lasers, Aussois, April 1986; J. Phys. (Paris) Colloq. **47**, C6-129 (1986).